34th Annual International Conference of the IEEE EMBS
San Diego, California USA, 28 August - 1 September, 2012

The kinematic architecture of the Active Headframe: a new head support for awake brain surgery

Matteo Malosio[1], Simone Pio Negri[1], Nicola Pedrocchi[1]
Federico Vicentini[1], Francesco Cardinale[2] and Lorenzo Molinari Tosatti[1]

***Abstract*— This paper presents the novel hybrid kinematic structure of the Active Headframe, a robotic head support to be employed in brain surgery operations for an active and dynamic control of the patient's head position and orientation, particularly addressing awake surgery requirements. The topology has been conceived in order to satisfy all the installation, functional and dynamic requirements. A kinetostatic optimization has been performed to obtain the actual geometric dimensions of the prototype currently being developed.**

I. INTRODUCTION

Brain surgery is reckoned as one of the oldest surgical practices, tracking back to the Neolithic age, with several different treated pathologies. Among them, epilepsy surgery is performed for reducing, possibly clearing, the onset of seizures in drug-resistant patients, who represent about the 30% of the epilepsy population [1]. Among these patients, those affected by focal seizures are paradigmatic candidates for epilepsy surgery. The overall prevalence of epilepsy in Europe is 8.23‰, with a recently recorded increasing trend (from 10,000 to 24,000 patients per year) in the number of candidates for epilepsy surgery. Considering procedural aspects, several routines (*e.g.* lesionectomies, temporal lobectomies, other monolobar or multilobar resections and/or disconnections, ...) require general anesthesia. However, seminal works in 1950s laid the groundwork for modern awake craniotomies [2], [3]. In selected clinical cases, in fact, awake-patient procedures help the operating team to map some critical brain areas, *e.g.* language. Intra-operative awake mapping is useful not only in some refractory epilepsy cases, but also in the surgical treatment of brain tumors, expecially low-grade gliomas [4]. Neurosurgical procedures, in general, require accurate and stable positioning and orienting of the patient's head. The Mayfield Headrest System [5], [6], named after his inventor in late 1960s, is the most commonly used head support, with some variations developed in recent years [7], [8]. It is a non-actuated head support, mechanically constrained in a given configuration by braked joints, adjusted by the neurosurgeon before registration. During procedures no modification of the head pose is usually planned, *i.e.* the head stays in the same pose w.r.t. the surgical bed for the entire operation. In awake surgery scenarios, a fixed device may cause patient's discomforts and, most importantly, it is impossible to control the amplitude and dampening of possible either natural or seizure-induced or stimulation-induced head motion and vibrations. In order to allow controlled movements of the head and improve the comfort of awake brain surgery operations, it is necessary to comply with a number of functional, kinematic and dynamic anatomical requirements, guaranteeing compatibility with typical surgery equipment. The paper presents the Active Headframe (hereafter AH) - a novel robotic six degrees-of-freedom (DoFs) head support - conceived, designed and optimized within the EU FP7 ACTIVE Project. The robot actively controls the patient's head position/orientation and dynamics throughout the whole surgical operation. In the following sections the AH innovative hybrid kinematic structure, its design highlights and some kinetostatic optimization results are presented. In particular, the relevant aspects here considered include the kinematic design process in relationship with functional requirements, the resulting range of motion (RoM) and joints decoupling, which is a very desirable property in control implementation. The paper is organized as follows: in section II all AH requirements and design guidelines are summarized, section III analytically reports the kinematic figures that are used in section IV for the kinetostatic optimization of the device in order to match the mechanical and functional objectives correlated to the requirements, before drawing conclusions in section V.

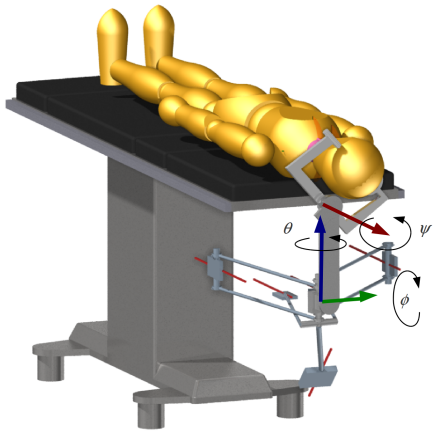

Fig. 1: A global rendered view of the AH, placed in its mounting position below the surgical bed. ϕ, θ and ψ represent the AH rotational degrees of freedom.

This work was partially supported by the European Commission with the Collaborative Project no. FP7-ICT-2009-6270460, ACTIVE: Active Constraints Technologies for Ill-defined or Volatile Environments.

[1]Matteo Malosio et al. are with the Institute of Industrial Technologies and Automation of the Italian National Research Council, via Bassini 15, 20133 Milan, Italy matteo.malosio at itia.cnr.it

[2]Francesco Cardinale is with the Niguarda Hospital, P.za Ospedale Maggiore 3, 20162 Milan, Italy

978-1-4577-1787-1/12/$26.00 ©2012 IEEE

II. AH REQUIREMENTS

In order to obtain a device efficiently employed during operations, the design of the AH kinematics has to satisfy different requirements: 1) fulfillment of surgical operations specifications, 2) compatibility with the patient's head RoM and 3) compatibility with other operating room equipment. Specifically, for standardization reasons and installation easiness, the AH adopts the largely-used Mayfield® clamp, as an end-effector rigidly coupled with the head (Fig. 1). In detail:

1) Application requirements: The AH has to provide a very stiff or, alternatively, compliant behaviour, depending on whether an accurately steady head positioning is required (*e.g.*in cranioctomy, electrostimulation,...) or compliant and adaptive motions are allowed - in control - for voluntary or involuntary (because of seizures) patient's head movements. Consequently, on one side the AH has to satisfy requirements in stiffness and precision, while on the other side an architecture characterized by low masses and inertias is desired in order to maximize dynamic performances.

2) Kinematic and dynamic requirements: The AH workspace has to be compatible with the anatomical RoM of the head. Specifically, even though the intra-operative expected RoM is relatively small around a balance pose, such pose can span over a large anatomical RoM due to the patient positioning on the bed[1]. Assuming that the patient's body is constrained onto the surgical bed, the head RoM can be decomposed in (i) the relative motion of the cervical vertebra C1 (*atlas*) with respect to C7 (*vertebra prominens*), assumed fixed w.r.t. the bed, and (ii) by the head skull rotation centered in C1 [9].
On the basis of the real human neck mobility [9] and of the actual surgical requirements [10], the AH required RoM has been defined as in Table I, where figures are referred to coordinates and frames defined in next section III. Additionally, the AH dynamic characteristics can be defined according to the anthropometric parameters and mass estimations available in [11], [12].

3) Footprint and compatibility to other equipment: The AH must be compatible with typical surgical beds, in terms of global footprint of the machine that has to be likely installed inside available free space below the bed. The AH footprint is required to be within the lateral bed boundaries and the patient's head projection on the ground (see Fig. 1). In this way, enough clearance for operating surgeons is preserved, together with available free space for additional equipment installation.

The design approach for meeting all the above listed requirements encompasses a hybrid-kinematic structure whose (i) parallel partially-decoupled kinematic architecture gives advantage for the stiffness and dynamics requirements and (ii) serial-kinematic joint is exploited for getting larger rotational RoM.

[1]The patient, wearing the Mayfield clamp detached from the AH, is positioned on the bed and *then* the device is set into the balance pose and the clamp assembled.

III. AH KINEMATICS

The AH hybrid kinematics includes a parallel architecture, which configures three translational and two rotational degrees of freedom (DoFs) of the mobile platform, and a serial axis provides the last rotational DoF (Figs. 2 and 3). The parallel part involves 5 kinematic chains, whose topology and sizes are optimized through kinetostatic indexes, see section IV. Such figures are of primary importance for the accuracy and the dynamic performances exploitable from the control layer. The following subsections report the design variables used in the optimization process: objective functions involve the Jacobian matrix, as a dominant kinetostatic relationship between the task domain (III-A, clinically relevant) and the joint domain (III-C), which in turn depends on the mechanical design of the parallel chains (III-B).

A. Coordinate frames and task-space coordinates

Let $O_f = [X_f, Y_f, Z_f]^T$ define the origin of a generic coordinate frame $\{f\}$ and $\{\mathbf{e}_{x,f}, \mathbf{e}_{y,f}, \mathbf{e}_{z,f}\}$ its coordinate axes unit vectors: in the following notation, $\{W\}$ denotes the base (world) reference, $\{e\}$ the frame of the AH (full mechanism) end-effector and $\{m\}$ is the frame of the mobile platform of the AH parallel mechanism (first 5 DoFs). The roto-translation in the task domain provided by the AH parallel part is:

$$ {}^W\mathbf{T}_m = \left[\begin{array}{c|c} Rot_y(\phi)Rot_z(\theta) & \begin{matrix} X_m \\ Y_m \\ Z_m \end{matrix} \\ \hline \mathbf{0} & 1 \end{array}\right] \tag{1} $$

where ${}^1\mathbf{T}_2$ is a homogeneous transform from frame $\{1\}$ to frame $\{2\}$ and its $Rot_u(\alpha)$ submatrix is a rotation in $\mathcal{SO}3$ given by an angle α about axis $\mathbf{u}$. The transform in (1) is given by the set $\mathbf{S}_m = [X_m, Y_m, Z_m, \phi, \theta]^T$ of the task-space DoFs that depends on the parallel part of the AH. The complete end-effector pose

$$ {}^W\mathbf{T}_e = {}^W\mathbf{T}_m \left[\begin{array}{c|c} Rot_x(\psi) & \begin{matrix} 0 \\ 0 \\ d_e \end{matrix} \\ \hline \mathbf{0} & 1 \end{array}\right] = {}^W\mathbf{T}_m {}^m\mathbf{T}_e \tag{2} $$

is given by the set $\mathbf{S}_e = [X_e, Y_e, Z_e, \phi, \theta, \psi]^T$, which includes the serial link coordinate ψ. Nevertheless, the distance d_e in (2) is constant so the serial link transform ${}^m\mathbf{T}_e = {}^m\mathbf{T}_e(\psi)$ depends only on rotation ψ in $\mathbf{S}_e$ and does not affect any kinetostatic property. The full set $\mathbf{S}_e$ is functionally required in order to provide the desired RoM (see Table I). However, being the kinetostatic and dynamical properties of the device derived from the topology of the parallel part, only $\mathbf{S}_m$ is elaborated in the following sections for the purpose of the optimization.

B. Design of parallel chains

All the parallel chains G_i, $i = 1, \ldots, 5$ as in Figs. 2 and 3, include struts L_i defined as

$$ L_i = Q_i - P_i \tag{3} $$

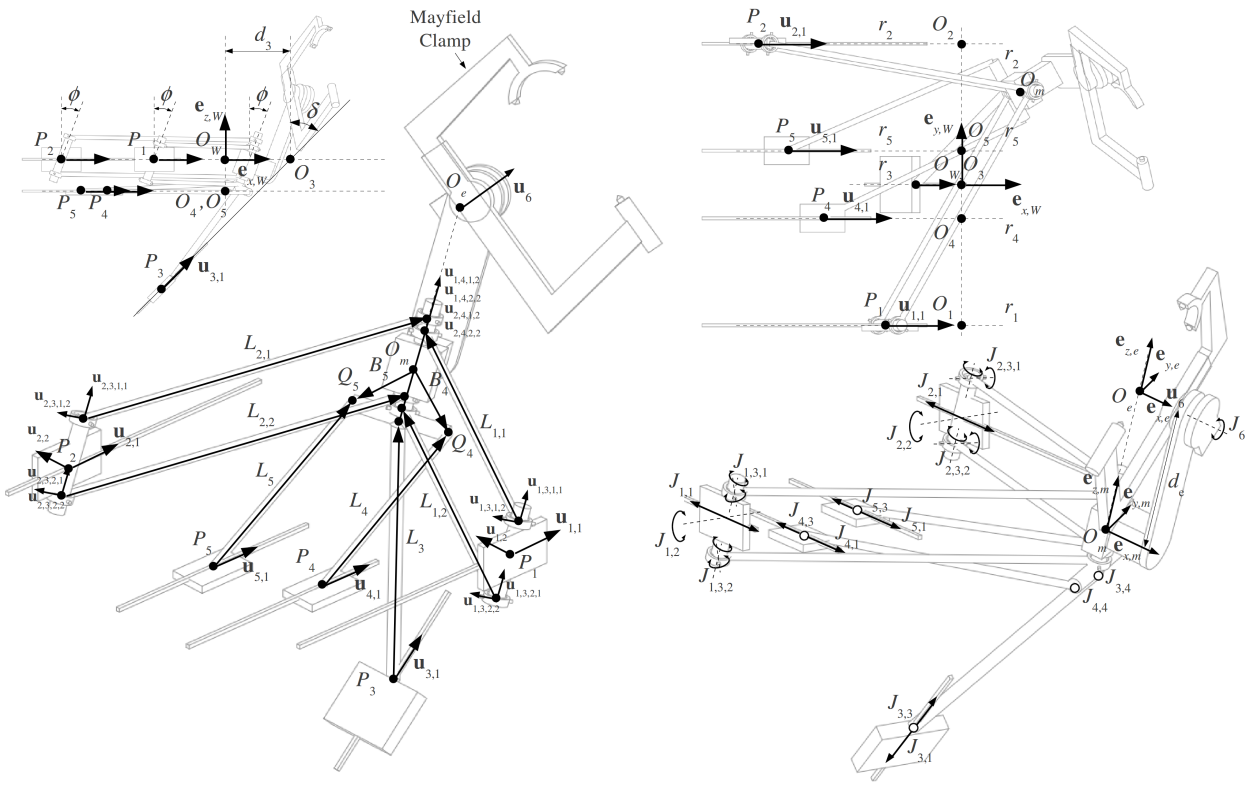

Fig. 2: Representation of the AH geometric and kinematic entities: (top left) lateral view, (bottom left) rear or "bed side" axonometric view, (top right) top view, (bottom right) front or "surgeon side" axonometric view (w.r.t. assembly in Fig. 1). $\mathbf{u}$ represents a joint axis of principal or sub- chains, intersecting at some O origins, P and Q points are the extremes of struts L in parallel chains. First subindex in all entities refers to $i = 1, \ldots, 5$ topologically represented in Fig. 3. Additional subindexes refer to sub-chains or additional mechanical components in the same chain.

TABLE I: ranges of AH task-space coordinates

DoF	min	max
X_e, Y_e, Z_e	-150 mm	150 mm
rotation ϕ	-20°	20°
rotation θ	-40°	40°
rotation ψ	-80°	80°

where $P_i = [X_{P,i}, Y_{P,i}, Z_{P,i}]^T$ is the i-th strut assembly point on its linear axis, $Q_i = O_m + B_i$ is the correspondent assembly point on the mobile platform and B_i is a proper offset of each strut w.r.t. the origin O_m.

Among all the chains, G_1 and G_2 are designed to have coupled constantly parallel struts $L_{1,1}//L_{1,2}$ and $L_{2,1}//L_{2,2}$ (denoting by $L_{i,j}$ the j-th strut of G_i) in order to increase the rotational stiffness of the mobile platform [13]. Struts $L_{1,1}$,$L_{1,2}$,$L_{2,1}$,$L_{2,2}$ are assembled at their ends by homokinetic pairs of Cardan joints, with parallel homologous axes (see Fig. 2). Such design conditions are:

$$\begin{cases} \mathbf{u}_{i,3,1,1} // \mathbf{u}_{i,4,1,2} // \mathbf{u}_{i,3,2,1} // \mathbf{u}_{i,4,2,2} \\ \mathbf{u}_{i,3,1,2} // \mathbf{u}_{i,4,1,1} // \mathbf{u}_{i,3,2,2} // \mathbf{u}_{i,4,2,1} \end{cases}$$

and

$$\begin{cases} \mathbf{u}_{i,3,1,1}, \mathbf{u}_{i,3,2,1} & \text{coaxial} \\ \mathbf{u}_{1,4,1,2}, \mathbf{u}_{1,4,2,2}, \mathbf{u}_{2,4,1,2}, \mathbf{u}_{2,4,2,2} & \text{coaxial} \end{cases}$$

$\forall i \in \{1, 2\}$. This makes the joints $J_{1,2}$ and $J_{2,2}$ (see Fig. 2) rotate around $\mathbf{u}_{1,2}$ and $\mathbf{u}_{2,2}$, respectively, by the same mobile platform angle $\phi \in S_m$ around $\mathbf{e}_{y,m}$, with the condition $\mathbf{u}_{1,3,1,1} // \mathbf{e}_{z,m} // \mathbf{u}_{2,3,1,1}$ constantly verified. Geometrically, struts in G_1 and G_2 are defined as

$$\begin{aligned} L_{i,j} = \quad & Q_i - P_i \\ & + (C_i + Rot_{\mathbf{e}_{y,m}}(\phi) C_j) \\ & - (C_i + Rot_{\mathbf{u}_{i,2}}(\phi) C_j) \end{aligned} \tag{4}$$

$\forall i, j \in \{1, 2\}$, where C_i and C_j are offset vectors designed for the struts assembly. Such geometrical representation is reported because, given the designed topology, the length of struts resulting from (3) and (4) is a key variable to be optimized on the basis of the kinetostatic properties of the kinematics.

C. Joint coordinates

The kinetostatic performances (see section IV) depend on the inverse kinematics Jacobian matrix $\mathbf{J}_m = \dot{Q}_m \dot{S}_m^{-1}$ [14],

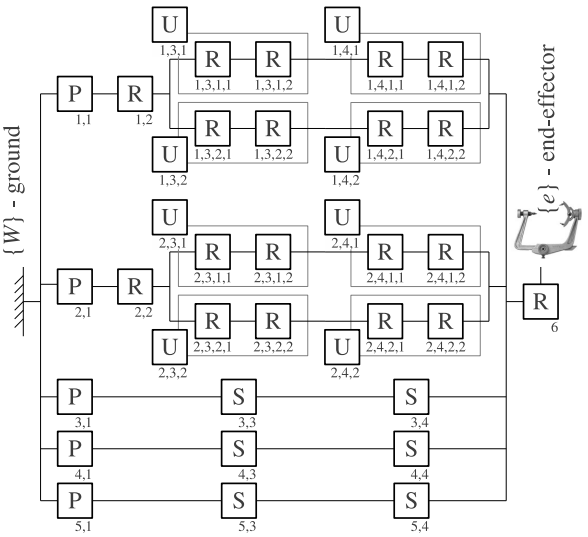

Fig. 3: Topology of the AH kinematics: horizontal branches depict the $i = 1, \ldots, 5$ parallel chains, each of which is composed by joints $J_{i,j,k,l}$ of type prismatic (P), rotational (R), universal (U) or spherical (S). Joint subindexes j,k,l refer to sub-chains or single elements belonging to the same i-th chain. Joints match the notation of their translation or rotational axis $\mathbf{u}_{i,j,k,l}$ represented in Fig. 2.

for which joint-space coordinates $\mathbf{Q}_m = [q_1, \ldots, q_5]^T$ have to be defined[2] from the designed geometry of the struts. In particular

$$q_i = \mathbf{u}_{i,1} \cdot (P_i - O_i) \qquad \forall i \in \{1, 2, 3, 4, 5\}, \tag{5}$$

where

$$\mathbf{u}_{i,1} = \begin{cases} [\sin\delta, 0, \cos\delta]^T & \text{if } i = 3 \\ [1, 0, 0]^T & \text{otherwise} \end{cases}$$

are the prismatic (actuated) joint axes.
The assembly points P_i and origins O_i in (5), through the struts length relations (3) and (4), are of primary importance for the design optimization because of their influence on both the Jacobian $\mathbf{J}_m$ and the definition of the reachable workspace. Procedurally, let r_i be the line, parametric in $t \in \mathbb{R}$, traced by the i-th linear joint:

$$r_i = \begin{cases} [d_3, 0, 0]^T + (\mathbf{e}_{x,W} \tan\delta + \mathbf{e}_{z,W})t & \text{if } i = 3 \\ [0, Y_{P,i}, Z_{P,i}]^T + \mathbf{e}_{x,W} t & \text{otherwise} \end{cases}$$

where $Y_{P,i}$,$Z_{P,i}$,d_3 are design-assigned values. Let then be p_{xy} and p_{yz} the planes defined by the unit vectors pairs $(\mathbf{e}_{x,W}, \mathbf{e}_{y,W})$ and $(\mathbf{e}_{y,W}, \mathbf{e}_{z,W})$, respectively. Then the joint origins to be used in (5) result to be

$$O_i = \begin{cases} r_i \cap p_{xy} & \text{if } i = 3 \\ r_i \cap p_{yz} & \text{otherwise.} \end{cases}$$

Then, being defined strut endpoint Q_i, the ground extreme P_i of each strut necessarily lies on the sphere s_i of radius r centered in Q_i, *i.e.*$s_i = \{P : \|P - Q_i\| = l_i\}$ where $l_i = \|L_i\|$ is the length of the struts. As a consequence

$$P_i = r_i \cap s_i \tag{6}$$

results in a quadratic equation to be considered, through the relationship in (5), in the design and optimization procedures. The condition in (6) has none, one or two real solutions, depending on the position of mobile platform, *i.e.* outside, on the boundary or inside the reachable workspace, respectively. Two distinct solutions represent two different assembly configurations.

IV. KINETOSTATIC OPTIMIZATION

The kinetostatic performances of the machine are usually analyzed through a set of jacobian-derived indexes that give a numerical evidence of some important physical/mechanical properties. In particular, such indexes are all built on the singular values σ of $\mathbf{J}_m$ computed in a set of sample configurations over the candidate workspace:

- the *manipulability* index, defined as $|\det(\mathbf{J}_m)|$, represents the overall stiffness of the mechanical structure;
- the *minimum stiffness* index, *i.e.* $\sigma_{min}(\mathbf{J}_m)$, represents the minimum stiffness;
- the *isotropy* index, defined as $\mathrm{cond}(\mathbf{J}_m) = {}^{\sigma_{max}}/_{\sigma_{min}}$, represents the highest-to-lowest stiffness ratio, resembling homogeneity of mechanical behavior.

The purpose of the optimization is to adjust links lengths and joints positions in order to improve the kinetostatic performances (affecting machine dynamics and control) preserving functional constraints. Such procedure was carried out exploiting the L-BFGS-B bound constrained optimization algorithm [15]. The imposed boundary conditions are set (see Table II) considering the available free-space below the surgical bed, *i.e.* matching requirements and limitations in the footprint of the device. Kinetostatic indexes are combined in order to achieve balanced performances and the cost function to be minimized is defined as [16]:

$$\chi = \lambda_1 \,\mathrm{cond}(J_m) + \frac{\lambda_2}{\sigma_{min}(J_m)} \quad \lambda_1 = 0.7, \lambda_2 = 0.3$$

for each point in which the workspace has been grid-discretized. The worst value χ among all the grid points, *i.e.* the worst pose/configuration, is retained at each optimization step. Optimized parameters, their boundary conditions and their optimal values are reported in Table III. The kinetostatic indexes evaluated in the discretized candidate workspace are shown in Fig. 4, assuming $\phi = 0$.

TABLE II: Constant parameters

Parameter	Value	Comment
$Y_{P,2} = -Y_{P,1}$	250 mm	To constrain the AH wide as the bed
δ	$\pi/4$	To avoid J_3 linear guides stand in the way of the surgeon's lower limbs
$\|\|B_3\|\|$	100 mm	Required offset for joints mechanical design and assembly reasons

[2]Full-mechanism joint variables are $\mathbf{Q}_e = [q_1, \ldots, q_6]^T$ with $q_6 = \psi$.

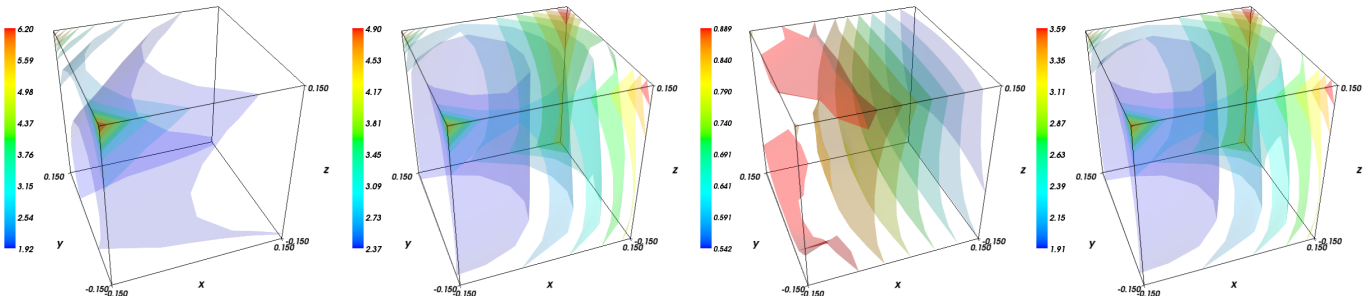

(a) Manipulability - $|\det(J)|$ (b) Conditioning - $\mathrm{cond}(J)$ (c) Lower stiffness - σ_{min} (d) Weighted kinetostatic index - χ

Fig. 4: Kinetostatic indexes of the optimized AH kinematic structure: (a)-(b)-(c) are single-index performance evaluations, (d) is the combined cost function. Specifically for (d), functions minimization (blue range) seeks for homogeneous behavior inside the workspace: red-range values are present only at boundaries of the workspace, where occurrence in positioning is negligible.

TABLE III: Optimized parameters

Parameter	min (mm)	max (mm)	optimum (mm)
$l_1 (= l_2)$	420	520	479
l_3	0	700	318
d_3	-150	250	180

V. CONCLUSIONS

The design of a robotic head support for awake surgery requires a high degree of accuracy and an inherently stiff mechanical behavior along all the machine configurations, a very compact footprint and a relatively large workspace. As a methodological framework, parallel kinematic machines allow a lightweight design, remarkable stiffness and fast dynamics. In addition, the workspace for head movements is required to be relatively large: in such case, the design outcomes could provide very poor kinetostatic performances in large portions of the mobile platform range. As a general guideline, in fact, singularities or a degraded manipulability or exceeding anisotropy should be avoided. For such reason, the design choices illustrated in the paper are devoted to decoupling translational and rotational motion components of the mobile platform, *i.e.* indirectly of the head. Similarly, the design choices aimed at supporting most of the bending loads through the usage of double struts. Such design considerations are partly used for the definition of the topology and for the device configuration, partly for the optimization of geometrical parameters. As a result, a combined set of values for the device components is found in order to provide a good trade-off between desired kinetostatic performances and required functional behavior and constraints. A detailed mechanical design of the AH is currently in progress and a patent application is in place.

REFERENCES

[1] J. F. Annegers, W. A. Hauser, and L. R. Elveback, "Remission of seizures and relapse in patients with epilepsy.," *Epilepsia*, vol. 20, pp. 729–737, Dec 1979.

[2] W. Penfield, "Combined regional and general anesthesia for craniotomy and cortical exploration. part i. neurosurgical considerations.," *Int Anesthesiol Clin*, vol. 24, no. 3, pp. 1–11, 1986.

[3] K. R. Bulsara, J. Johnson, and A. T. Villavicencio, "Improvements in brain tumor surgery: the modern history of awake craniotomies," *Neurosurgical Focus*, vol. 18, no. 4, pp. 1–3, 2005.

[4] H. Duffau, "The necessity of preserving brain functions in glioma surgery: the crucial role of intraoperative awake mapping," *World Neurosurgery*, vol. 76(6), pp. 525–527, 2011.

[5] H. R. Hickmann, "Surgical head clamp," 1979.

[6] J. L. Day and C. Dinkler, "Surgical head clamp," 1993.

[7] J. L. Day and D. A. Lincoln, "Skull clamp with load distribution indicators," 2007.

[8] C. E. Dinkler and K. R. Easton, "Head support system," 2006.

[9] V. Zatsiorsky, *Kinematics of Human Motion*. Human Kinetics, 1 ed., Sept. 1997.

[10] A. L. Rhoton, "Operative techniques and instrumentation for neurosurgery.," *Neurosurgery*, vol. 53, Oct. 2003.

[11] V. M. Zatsiorsky and V. Seluyanov, "Mass and inertia characteristics of the main segments of the human body," *International Series on Biomechanics*, vol. 4B, pp. 1152–1159, 1983.

[12] P. De Leva, "Adjustments to zatsiorsky-seluyanov's segment inertia parameters," *Journal of Biomechanics*, vol. 29, no. 9, pp. 1223 – 1230, 1996.

[13] S. P. Negri, L. Molinari Tosatti, and I. Fassi, "Improvement and optimization of a reconfigurable parallel kinematic machine," in *Proceedings of JUSFA 2002 Japan-USA Symposium on Flexible Automation*, (Hiroshima, Japan), 2002.

[14] J. Angeles, *Fundamentals of Robotic Mechanical Systems: Theory, Methods, and Algorithms*. Springer, 2007.

[15] R. H. Byrd, P. Lu, J. Nocedal, and C. Zhu, "A limited memory algorithm for bound constrained optimization," *SIAM J. Sci. Comput.*, vol. 16, pp. 1190–1208, Sept. 1995.

[16] G. Antonelli, F. Caccavale, and P. Chiacchio, "A systematic procedure for the identification of dynamic parameters of robot manipulators," *Robotica*, vol. 17, no. 04, pp. 427–435, 1999.